Excess Noise Factors for Conventional and Superlattice Avalanche Photodiodes and Photomultiplier Tubes

MALVIN C. TEICH, SENIOR MEMBER, IEEE, KUNIAKI MATSUO, MEMBER, IEEE, AND BAHAA E. A. SALEH, MEMBER, IEEE

Abstract—**Light falling on a photodetector produces an output current that fluctuates. The noise in this signal arises from two sources: randomness in the photon arrivals and randomness in the carrier multiplication process intrinsic to the photodetector. A general formula is derived for the variance of the photodetector output current in terms of parameters characterizing these two sources of randomness (the photon-number variance-to-mean ratio for the light and the excess noise factor for the detector). An important special case of this formula illustrates that the output-current variance is directly proportional to the detector excess noise factor when the number of photons at the input to the detector is Poisson distributed. Explicit expressions for excess noise factors are provided for three kinds of photodetectors: the double-carrier conventional avalanche photodiode, the double-carrier superlattice avalanche photodiode, and the photomultiplier tube. The results for the double-carrier superlattice device are new; it is shown that even a small amount of residual hole ionization can lead to a large excess noise factor. Comparisons are drawn among the detectors in terms of their noise properties.**

I. Introduction

LIGHT falling on a photodetector produces an output current that fluctuates. The noise in this signal arises from two sources: randomness in the photon arrival number and randomness in the carrier multiplication process intrinsic to the photodetector. The object of this paper is fourfold. First, we calculate the variance of the output current in terms of parameters that characterize these two sources of randomness (the Fano factor for the light and the excess noise factor for the detector multiplication process). Second, we demonstrate that in the usual situation (Poisson photon arrivals), a simple relation between the output-current variance and the excess noise factor of the multiplication ensues. Third, we give explicit expressions for the excess noise factors of three photodetectors of interest: the conventional avalanche photodiode, the superlattice avalanche photodiode, and the photomultiplier tube. Finally, we compare and contrast the noise behavior of these three photodetectors, illustrating their relative merits.

The usual method for experimentally determining the excess noise factor for an APD involves a measurement of the variance of the output current[1] when the device is illuminated by a Poisson stream of photons [1]. Yet the theoretically calculated excess noise factor is defined in terms of the normalized second moment of the gain random variable when a single photocarrier initiates the multiplication [2]–[4]. The relationship between the two quantities is generally obtained individually for each APD [2]–[5]. Our first task is to derive a general formula that relates these quantities for an arbitrary source of light and for an arbitrary detector multiplication process. When the number of photons at the input to the detector is Poisson, the output-current variance turns out to be directly proportional to the excess noise factor.

Explicit formulas for the excess noise factor are presented for several special cases: the conventional avalanche photodiode (CAPD), the superlattice avalanche photodiode (SAPD), and the photomultiplier tube (PMT). The results for the CAPD are in accord with the expressions obtained earlier by McIntyre [2], [3], whereas the results for the single-carrier SAPD agree with those reported by Capasso *et al.* [5] for the graded-gap staircase APD. The expressions for the double-carrier SAPD are new, although they are related to expressions obtained by van Vliet *et al.* [6]. The formulas for the PMT were derived long ago by Zworykin *et al.* [7] and by Shockley and Pierce [8]. The noisiness of the three photodetectors is compared graphically.

The excess noise factor is a useful statistic because it represents, in a compact way, the lowest order statistical properties of the gain fluctuations that introduce multiplicative noise. However, it must be recognized that, aside from photon fluctuations, the excess noise factor does not provide a complete statistical description of the electron current. While it is useful for the calculation of quantities such as the conventional signal-to-noise ratio (SNR) for

Manuscript received December 27, 1985. This research was supported by the National Science Foundation.

M. C. Teich is with the Columbia Radiation Laboratory and the Center for Telecommunications Research, Department of Electrical Engineering, Columbia University, New York, NY 10027.

K. Matsuo was with the Columbia Radiation Laboratory, Department of Electrical Engineering, Columbia University, New York, NY 10027. He is now with the Hiroshima-Denki Institute of Technology, Hiroshima, Japan.

B. E. A. Saleh is with the Department of Electrical and Computer Engineering, University of Wisconsin, Madison, WI 53706.

IEEE Log Number 8608891.

[1]If only the ac or "signal" portion of the current is considered, the variance is equivalent to the mean-square current.

0018-9197/86/0800-1184$01.00

analog detection, it is inadequate for describing the performance of a digital-signal information transmission system [9]. Instead, measures such as probability of detection and probability of error must be used for such systems. These latter quantities are strongly dependent on the tails of the counting distributions (beyond the second moment) and therefore require a more complete statistical description of the electron current (e.g., the counting distribution) [10]–[12].

II. Theory

Consider a point process representing the primary (photon-generated) carriers. Let the number of these carriers generated within the time interval $[0, T]$ be described by the discrete random variable a. Each of these primary carriers, in turn, is assumed to independently produce M daughter carriers (M is the discrete gain random variable representing the carrier multiplication). The total number of electrons n produced at the output of the device is the quantity of interest.

If a and M are statistically independent, which it is safe to assume, then

$$\langle n \rangle = \langle M \rangle \langle a \rangle \tag{1}$$

and

$$\text{Var}\,(n) = \langle M \rangle^2 \,\text{Var}\,(a) + \langle a \rangle \,\text{Var}\,(M). \tag{2}$$

The angular brackets $\langle \cdot \rangle$ represent the ensemble average and Var $(\cdot)$ represents the count variance. These relationships are known as the Burgess variance theorem [13]–[15]. Dividing (2) by (1) provides

$$\mathcal{F}_n = \langle M \rangle \mathcal{F}_a + \mathcal{F}_M \tag{3}$$

where the Fano factors $\mathcal{F}_j$ are defined as

$$\mathcal{F}_j = \text{Var}\,(j)/\langle j \rangle, \qquad j = n, a, M. \tag{4}$$

The quantity $\mathcal{F}_a$ is the Fano factor for the photogenerated carriers. For many photon-counting distributions, including the Poisson, the Fano factor is invariant to random deletion [14], in which case $\mathcal{F}_a$ is the same as the Fano factor for the photons incident on the device ($\mathcal{F}_{\text{photon}}$). Equation (3) is are then independent of the detector quantum efficiency η.

In many detectors, the processes a and n are filtered (continuous) versions of their discrete counterparts. In that case, we use the spectral form of the Burgess variance theorem [15]

$$\langle I_n \rangle = \langle M \rangle \langle I_a \rangle \tag{5}$$

and

$$S_n = \langle M \rangle^2 S_a + 2q \langle I_a \rangle \,\text{Var}\,(M). \tag{6}$$

The quantities $\langle I_n \rangle$ and $\langle I_a \rangle$ and S_n and S_a represent the mean currents and power spectral densities, respectively, for the n and a processes; q is the electronic charge. Since the primary process satisfies

$$\text{Var}\,(I_a) = (q/T)^2 \,\text{Var}\,(a), \tag{7}$$

the relation $B = 1/2T$ (where B is the bandwidth of the system) can be used to obtain

$$S_a = 2q \langle I_a \rangle \mathcal{F}_a, \tag{8a}$$

thereby allowing (6) to be simplified to

$$S_n = 2q \langle I_a \rangle [\langle M \rangle^2 \mathcal{F}_a + \text{Var}\,(M)]. \tag{8b}$$

The excess noise factor F_e is defined as the normalized second moment of the gain random variable *for a single input photocarrier*, i.e.,

$$F_e = \langle M^2 \rangle / \langle M \rangle^2. \tag{9}$$

Equation (9) can be used in conjunction with (8) to provide

$$S_n = 2q \langle I_a \rangle \langle M \rangle^2 [\mathcal{F}_a + (F_e - 1)] \tag{10a}$$

and

$$\text{Var}\,(I_n) = 2q \langle I_a \rangle B \langle M \rangle^2 [\mathcal{F}_a + (F_e - 1)], \tag{10b}$$

which is the desired general relationship. Combining (9) with (2) leads to the discrete analog to (10b), which may be written as

$$\text{Var}\,(n) = \langle a \rangle \langle M \rangle^2 [\mathcal{F}_a + (F_e - 1)] \tag{10c}$$

or equivalently as

$$\mathcal{F}_n = \langle M \rangle [\mathcal{F}_a + (F_e - 1)]. \tag{10d}$$

The excess noise factor can also be expressed in terms of the mean and variance of the gain by

$$F_e = 1 + [\text{Var}\,(M)/\langle M \rangle^2]. \tag{11}$$

For deterministic multiplication

$$\text{Var}\,(M) = 0, \qquad F_e = 1 \tag{12}$$

whence the name "excess noise factor."

The laboratory measurement of an experimental excess noise factor ϕ_e is often carried out by determining the true ac mean-square current at the output of the APD under study and the true ac mean-square current at the output of a device identical in all respects except that with unity multiplication. The ratio of these two currents (which are, properly speaking, variances) provides the experimental excess noise factor ϕ_e [1]. We therefore have

$$\phi_e = \text{Var}\,(I_n)/\text{Var}\,(I_a) = S_n B / S_a B. \tag{13}$$

Using (10a) together with (8a) leads to

$$\phi_e = (\langle M \rangle^2 / \mathcal{F}_a) [\mathcal{F}_a + (F_e - 1)]. \tag{14a}$$

Actual experimental measurements of ϕ_e are invariably carried out with a source of radiation that generates a Poisson flow of photocarriers. In that case, $\mathcal{F}_a = 1$ so that (14a) becomes

$$\phi_e = \langle M \rangle^2 F_e. \tag{14b}$$

This explicitly demonstrates the proportionality of the experimentally determined and theoretically calculated excess noise factors for Poisson light.

The general result for ϕ_e given in (14a) may be equiv-

alently expressed in terms of the mean $\langle M \rangle$ and Fano factors $\mathcal{F}_M$ and $\mathcal{F}_a$. Using (11), we obtain

$$\phi_e = \langle M \rangle (\langle M \rangle + \mathcal{F}_M/\mathcal{F}_a). \tag{15a}$$

In the case of Poisson photocarriers, this simplifies to

$$\phi_e = \langle M \rangle (\langle M \rangle + \mathcal{F}_M). \tag{15b}$$

III. Excess Noise Factor for the Conventional APD

An expression for the excess noise factor F_e associated with avalanching in a uniformly multiplying p-n junction was first derived by McIntyre [2]. When only electrons are injected into the depletion layer, but both electrons and holes have the capability to impact ionize, the result can be written as

$$F_e \text{ (electron injection)} = [k_c\langle M \rangle + (2 - 1/\langle M \rangle)(1 - k_c)]; \tag{16a}$$

when only holes are injected, it becomes

$$F_e \text{ (hole injection)} = [\langle M \rangle/k_c - (2 - 1/\langle M \rangle)(1 - k_c)/k_c]. \tag{16b}$$

Equations (16a) and (16b) are, as indicated above, valid for single-carrier-initiated/double-carrier multiplication (SCIDCM). The quantity

$$k_c = \beta/\alpha \tag{17}$$

in (16a) and (16b) represents the ratio of hole-ionization probability per unit length β to electron-ionization probability per unit length α. This ratio is assumed to be independent of the electric field $\vec{E}$ and constant throughout the avalanche region.[2] Equation (16b) may be obtained directly from (16a) by using the substitution $k_c \rightarrow 1/k_c$. If electrons and holes are both injected, the overall result is obtained by adding the two partial results.[2] The lower the value of k_c, the lower the device noise. In experimentally determining the APD excess noise factor, the quantity that is directly measured is the variance of the output current in response to a Poisson stream of photons at the input, as specified in (10b) with $\mathcal{F}_a = 1$. Using (16a) and (16b) in (10b) provides results that accord with those derived by McIntyre [2].

The average multiplication (mean gain) $\langle M \rangle$ for a CAPD with pure electron injection, expressed as a function of the distance from the edge of the depletion layer x, is [2]–[4]

$$\langle M \rangle = (1 - k_c)/\{\exp[\alpha(k_c - 1)x] - k_c\}, \qquad k_c \neq 1. \tag{18}$$

[2]McIntyre [3] demonstrated that even if β is not proportional to α, a suitable value for k_c, called k_{eff}, can be defined for F_e if $\langle M \rangle$ is large. Furthermore, additional noise is introduced when light is absorbed on both sides of the junction, so that both electrons and holes are injected into the avalanche region (this is double-carrier-initiated/double-carrier multiplication or DCIDCM). In that case, an effective excess noise factor F_{eff} can be defined [4]. McIntyre's theoretical results for Si APD's were experimentally verified by Conradi [1].

The performance of digital-communication systems incorporating CAPD's was examined in detail by Personick. His initial treatment of this topic [10] dealt with multiplication involving a single ionizing carrier, as well as multiplication involving two carriers with equal ionization coefficients. In a subsequent generalization [11], he obtained upper-bound performance results for double-carrier devices with unequal ionization coefficients. Personick's results are consistent with those obtained by McIntyre [3].

An important special case is that of the CAPD under single-carrier-initiated/single-carrier multiplication (SCISCM) conditions. This provides the lowest possible noise. Setting $k_c = 0$ in (16a) or $k_c = \infty$ in (16b) leads to

$$F_e = 2 - 1/\langle M \rangle \tag{19}$$

which, with the help of (10b) with $\mathcal{F}_a = 1$, gives rise to

$$\text{Var}(I_n) = 2q\langle I_a \rangle B\langle M \rangle [2\langle M \rangle - 1]. \tag{20}$$

The average multiplication, readily obtained from (18), is then

$$\langle M \rangle = \exp(\alpha x). \tag{21}$$

Inserting (21) into (20) gives the expression for the variance of a filtered Yule–Furry birth process with a Poisson initial population [16]. The identity between the statistics of the SCISCM CAPD and the Yule–Furry process is confirmed by the gain distribution (in response to a single initiating event); it is the shifted Bose–Einstein distribution in both cases [10], [12], [16].

In the case where the ionization coefficients for electrons and holes are equal ($\alpha = \beta$; $k_c = 1$), (16a) and (16b) become

$$F_e = \langle M \rangle, \tag{22}$$

whereupon (10b), with $\mathcal{F}_a = 1$, provides

$$\text{Var}(I_n) = 2q\langle I_a \rangle B\langle M \rangle^3, \tag{23}$$

as first obtained by Tager [17]. The average multiplication is then

$$\langle M \rangle = 1/(1 - \alpha x), \qquad k_c = 1. \tag{24}$$

For a device operated with either pure-electron or pure-hole delta-function injection (i.e., pure injection at one or the other edge of the depletion layer), this is the noisiest situation. However, for $\alpha \neq \beta$, F_e can be even greater than or less than $\langle M \rangle$, depending on where the light is absorbed in the junction.[2]

IV. Excess Noise Factor for the Superlattice APD

An illustrative example of a superlattice APD (SAPD) is the staircase avalanche photodiode. It is a graded-gap multilayer device proposed by Williams, Capasso, and Tsang [5], [18], [19] for low-noise light detection in the near-infrared region of the spectrum. The device is of interest for fiber-optic communications. It is designed to achieve an enhancement of the impact-ionization proba-

bility ratio, thereby minimizing the hole-electron feedback noise associated with conventional III–V quaternary APD's for which $k_c \approx 1$ [20]. Furthermore, because the electron multiplication can occur only at a finite number of discrete locations in the device, the variability of the number of electrons generated per detected photon is also reduced relative to the CAPD. (It has already been experimentally shown that the first superlattice APD structure, proposed by Chin *et al.*, can provide an enhanced ionization ratio [21]–[25].) The fabrication of a staircase device in this region of the spectrum, using molecular-beam epitaxy, is currently underway at AT&T Bell Laboratories [24].

Although we deal with the graded-gap staircase SAPD extensively for purposes of illustration, the analysis presented here is applicable for any SAPD in which the carrier transport is perpendicular to the superlattice planes. In such structures, the carriers encounter a potential discontinuity at the heterointerfaces at each period of the multilayer structure. Thus, our results will also apply to the multiquantum-well SAPD structure of Chin *et al.* [21]–[23], [25], the doped-quantum-well SAPD structure of Blauvelt *et al.* [26], and the stored-carrier multiquantum-well SAPD [27]–[29]. However, the results will not apply to the channeling APD [30], [31], nor to other devices in which the carriers are spatially separated by means of a transverse field with transport taking place in the plane of the layers.

The gain, excess noise factor, and electron probability distribution at the output of a staircase SAPD have recently been calculated as a function of the number of stages of the device m and the electron impact-ionization probability per stage P under the SCISCM assumption [32].[3] This analysis is valid not only for the staircase SAPD, but for any of the perpendicular-carrier-transport SAPD's.

We now extend these results to allow for residual hole-initiated ionization in the graded regions of the device, arising from the applied electric field. (The valence-band steps are of the wrong sign to assist hole-initiated ionization; indeed they may lead to hole trapping. Also, because of the opposing conduction-band quasi-electric field, the electrons can impact ionize only at the conduction-band discontinuities.) The mathematical results follow from the treatment provided by van Vliet *et al.* [6], with appropriate extension and reinterpretation. The model provided by these authors was intended to describe multiplication noise in CAPD's. However, their use of a deterministic number of shifted-Bernoulli stages makes their model a good starting point for describing the excess noise factor for the double-carrier instantaneous-multiplication SAPD. Although the theory is appropriate as it stands for those SAPD's in which both electron and hole ionizations occur at discrete locations (e.g., the multiquantum-well SAPD [23]), it must be modified for the staircase SAPD. In this latter case, we must incorporate a proper *continuous* theory for the hole-ionization probability [5] into the discrete shifted-Bernoulli theory of van Vliet *et al.*

The excess noise factor F_e for the double-carrier SAPD with electron injection may then be obtained from the expression for the variance derived by van Vliet *et al.* [6, eq. (73)] using the notational replacements $M_N \rightarrow \langle M \rangle$, $\lambda \rightarrow P$, and $k \rightarrow k_s$ along with (11). This yields

$$F_e \text{ (electron injection)} = 1 + \frac{(1 - 1/\langle M \rangle)(1 - k_s)}{2 + P(1 + k_s)} \times \left\{ -P + 2\,\frac{1 - k_s P^2}{1 + k_s P}\left[\langle M \rangle\, k_s \frac{1 + P}{1 - k_s} + \frac{1}{1 + P} \right] \right\}. \tag{25}$$

As previously, P is the electron impact-ionization probability per stage and $\langle M \rangle$ is the average overall multiplication for the device. The ratio of the hole-ionization probability per stage Q to the electron-ionization probability per stage P defines k_s for the SAPD, i.e.,

$$k_s = Q/P. \tag{26a}$$

For the staircase SAPD, Q is given by [5]

$$Q = \exp\left(\int_0^L \beta\, dz \right) - 1 \tag{26b}$$

where β is the hole-ionization coefficient (probability per unit length) in the graded region and L is the length of each stage.

The average multiplication $\langle M \rangle$ is obtained with the help of [6, eq. (53)] and (26a) which, together with the notational substitutions $\lambda \rightarrow P$, $\mu \rightarrow Q$, $N \rightarrow m$, yield

$$\langle M \rangle = \frac{(1 + P)^m (1 - k_s)}{(1 + k_s P)^{m+1} - k_s (1 + P)^{m+1}}. \tag{27}$$

From (27), it is apparent that the expression for the excess noise factor in (25) could readily be expressed as a function of P, k_s, and m instead of P, k_s, and $\langle M \rangle$. When $k_s \neq 0$, the average multiplication in (27) will increase without limit for certain parameter values (i.e., avalanche breakdown will occur). The validity of (27) is restricted to the parameter space below avalanche breakdown.

The modified excess noise factor $(F_e - 1)$ for the SCIDCM SAPD is plotted as a function of the average multiplication $\langle M \rangle$ with the help of (25) and (27). The modified excess noise factor is used because it is conveniently displayed on double-logarithmic coordinates. Furthermore, as is evident from Section II, it is the pertinent measure in the absence of quantum fluctuations. In Figs. 1 and 2, we illustrate its behavior for $m = 3$ and 10, respectively. Results for several values of k_s are presented

[3]The impulse response function was also calculated by incorporating the effects of (random) transit time into the carrier multiplication process.

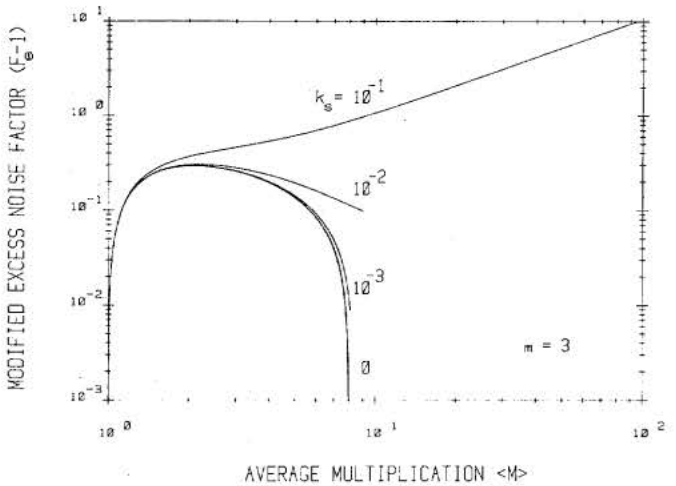

Fig. 1. Modified excess noise factor $F_e - 1$ versus average multiplication $\langle M \rangle$ for the single-carrier-initiated/double-carrier multiplication (SCIDCM) SAPD. The modified excess noise factor is plotted because it can be conveniently displayed on double-logarithmic coordinates. It is the pertinent measure in the absence of quantum fluctuations. The number of stages $m = 3$. The behavior for different values of k_s is illustrated parametrically. The curve for $k_s = 0$ corresponds to the single-carrier-initiated/single-carrier multiplication (SCISCM) SAPD. It is apparent that even small deviations of k_s from 0 result in substantial excess noise.

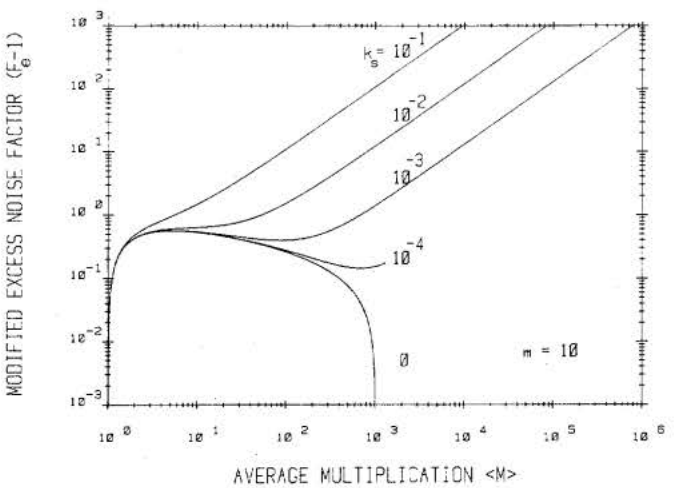

Fig. 2. Modified excess noise factor $F_e - 1$ versus average multiplication $\langle M \rangle$ for the SCIDCM SAPD with $m = 10$. Again, the curve $k_s = 0$ corresponds to the SCISCM SAPD. Comparison to Fig. 1 demonstrates that as m increases, the deleterious effects of residual hole ionization become more pronounced.

parametrically. The $k_s = 0$ curve corresponds to the SCISCM SAPD. As for the CAPD, the lower the value of k_s, the lower the noise. It is apparent that even small deviations of k_s from 0 result in substantial excess noise. This effect is more pronounced as m increases. These results provide limits on the residual hole ionization that is tolerable in an SAPD. Based on a many-particle Monte Carlo simulation, Brennan [33] has recently estimated k_s to be $\approx 10^{-1}$ for the multiquantum-well SAPD of Chin *et al.* [23] and $\approx 10^{-2}$ for the staircase SAPD of Williams *et al.* [18], in the GaAs/AlGaAs system. He has also shown that even lower values of k_s may be achievable by using the doped-quantum-well SAPD structure of Blauvelt *et al.* [26].

The most important special case, of course, is that of the SCISCM device, which is the lowest noise SAPD. From (27), the average multiplication for the single-carrier multiplication SAPD is easily shown to be

$$\langle M \rangle = (1 + P)^m. \tag{28}$$

The excess noise factor is obtained by setting $k_s = 0$ in (25), which leads to

$$F_e = 1 + [(1 - P)/(1 + P)][1 - (1 + P)^{-m}] \tag{29a}$$

$$= \langle M \rangle^{-1} + 2\langle M \rangle^{-1/m} - 2\langle M \rangle^{-1-1/m}. \tag{29b}$$

Using (14b), the experimental excess noise factor ϕ_e will then be given by

$$\phi_e = (1 + P)^{2m} + [(1 - P)/(1 + P)][(1 + P)^{2m} - (1 + P)^m] \tag{30}$$

which, with the help of (10b) and $\mathfrak{F}_a = 1$, corresponds to the output current variance

$$\text{Var}\,(I_n) = 2q\langle I_a \rangle B\{(1 + P)^{2m} + [(1 - P)/(1 + P)] \cdot [(1 + P)^{2m} - (1 + P)^m]\}. \tag{31}$$

Equation (29a) agrees with the formula obtained by Capasso *et al.* [5, eq. (2)]. Equation (31) is also in accord with their result [5, eq. (1)], provided that the quantity $\langle i^2 \rangle$ in [5, eq. (1)] is interpreted as the power spectral density S_n. All of the formulas presented here are in agreement with those reported in [32]. Equation (29b) is displayed in Figs. 1 and 2 ($k_s = 0$).

Carrying (29b) to the limit $m \to \infty$ leads to the result

$$F_e = 2 - 1/\langle M \rangle, \tag{32}$$

which is identical to that given for the SCISCM CAPD in (19). This is as expected; in this limit, there is an infinite number of stages and the probability is vanishingly small that a carrier is produced by impact ionization in any one given stage of the device.

Finally, we consider the case of equal ionization coefficients for electrons and holes in the SAPD ($P = Q$; $k_s = 1$). The excess noise factor, output-current variance, and average multiplication then become

$$F_e = \langle M \rangle - (\langle M \rangle - 1)^2/m\langle M \rangle \tag{33}$$

$$\text{Var}\,(I_n) = 2q\langle I_a \rangle B[\langle M \rangle^3 - \langle M \rangle(\langle M \rangle - 1)^2/m] \tag{34}$$

and

$$\langle M \rangle = 1/(1 - Pm), \tag{35}$$

respectively. Carrying (33) to the limit $m \to \infty$ provides

$$F_e = \langle M \rangle \tag{36}$$

which is identical to the SCIDCM CAPD result given in (22) for the same reasons as indicated above.

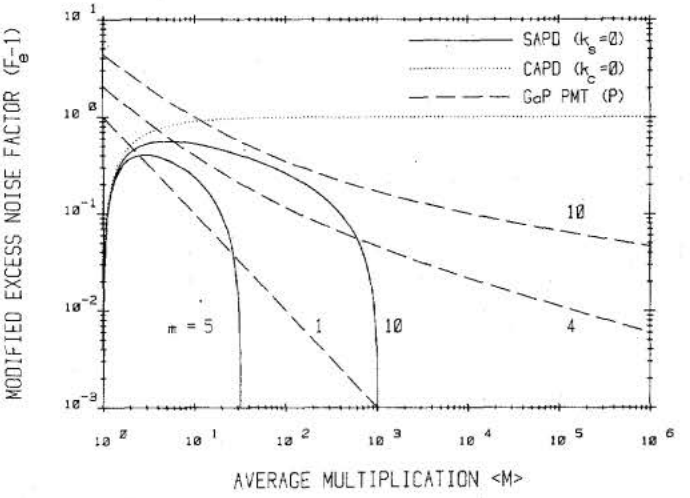

Fig. 3. Modified excess noise factor $F_e - 1$ versus average multiplication $\langle M \rangle$ for the SCISCM SAPD (solid curves) with $m = 5$ and 10, the SCISCM CAPD (dotted curve), and the high-gain GaP-first-dynode PMT with Poisson multiplication and $A = 10$ (dashed curves) for $m = 1$, 4, 10. This figure illustrates the best possible behavior for all three devices. Although the theoretical excess noise factor of the SAPD is always superior to that of the CAPD, the differential cannot be large because $F_e < 2$ for both devices. The PMT exhibits high-gain, low-noise behavior for all useful values of $\langle M \rangle$. In terms of the excess noise factor, it can exhibit better performance than the SAPD.

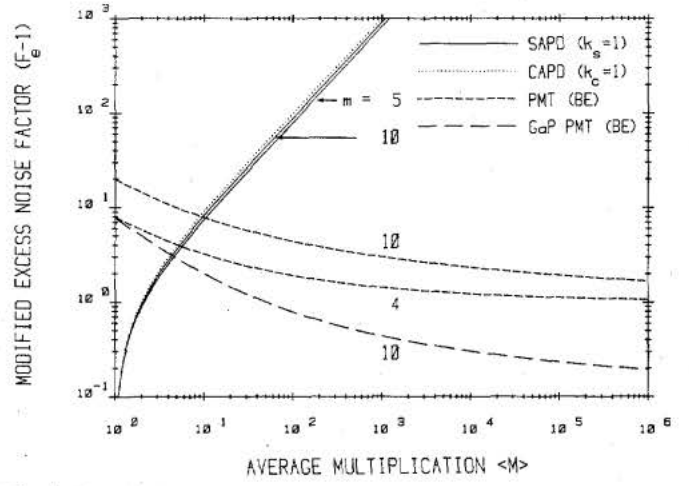

Fig. 4. Modified excess noise factor $F_e - 1$ versus average multiplication $\langle M \rangle$ for the SCIDCM SAPD ($k_s = 1$, solid curves) with $m = 5$ and 10, the SCIDCM CAPD ($k_c = 1$, dotted curve), the identical-dynode PMT with Bose–Einstein multiplication (short-dash curves) and with $m = 4$ and 10, and the high-gain GaP-first-dynode 10-stage PMT with Bose–Einstein multiplication and with $A = 10$ (long-dash curve). This figure illustrates the worst possible behavior for all three devices, assuming single carrier (delta-function) injection. For the CAPD, F_e is identically equal to $\langle M \rangle$, whereas for the SAPD, F_e increases approximately as $\langle M \rangle$. These results illustrate explicitly that the feedback associated with double-carrier multiplication in APD's gives rise to far more noise than does uncertainty in the ionization locations. The quintessentially single-carrier PMT displays far and away the lowest values of the excess noise factor.

V. Comparison of Excess Noise Factors for the SAPD and the CAPD

The modified excess noise factors for the SAPD (solid curves) and CAPD (dotted curves) are plotted versus the average multiplication $\langle M \rangle$ in Figs. 3 and 4 for $k_s = k_c = 0$ and $k_s = k_c = 1$, respectively. The results in Fig. 3 are for SCISCM conditions, representing the best possible behavior of both devices. The excess noise factors for both the SAPD and the CAPD then always lie below 2, as is apparent from (19) and (29a). Although the theoretical performance of the SAPD is always superior to that of the CAPD, the differential (in terms of excess noise factor) cannot be very large since $F_e < 2$ for both cases.

In the opposite limit (SCIDCM with equal impact-ionization probabilities), the results are displayed in Fig. 4. This is the worst possible behavior for both devices, assuming single-carrier (delta-function) injection. F_e for the CAPD is identically $\langle M \rangle$ from (22). F_e for the SAPD also increases in approximate proportion to $\langle M \rangle$, but with the coefficient $(1 - 1/m)$, which is slightly below unity, as can be discerned from (33). Thus, the SAPD excess-noise curves lie slightly below the CAPD curve for finite m, coming ever closer as $m \to \infty$, in accord with (36).

The results presented in Figs. 3 and 4 illustrate explicitly that the feedback noise introduced by the process of double-carrier multiplication is far more deleterious to noise performance than is the randomness associated with uncertainty in the locations of the ionizations.

VI. Excess Noise Factor for the Photomultiplier Tube

The photomultiplier tube (PMT) is one of the oldest and most versatile of light detectors, having been developed about 1935 [7]. From a noise point of view, it has the distinct advantage of being a single-carrier device (SCISCM) since the electrons travel in vacuum. An excellent description of essentially all aspects of PMT operation is available in the *RCA Photomultiplier Handbook* [34]; in particular, the reader is directed to Appendix G (pp. 160–176) for a comprehensive discussion of the statistical theory of PMT noise.

The average multiplication for an m-stage device is given by [34, eq. (G-55)]

$$\langle M \rangle = \prod_{k=1}^{m} \langle \delta_k \rangle \tag{37}$$

where $\langle \delta_k \rangle$ is the mean secondary-emission gain at the kth stage. The random variable δ_k represents the kth-stage secondary-emission gain. Using an expression for the variance of the multiplication M at the output of the PMT [34, eq. (G-56)] together with (11) gives the excess noise factor

$$F_e = 1 + \frac{\text{Var}\,(\delta_1)}{\langle \delta_1 \rangle^2} + \frac{\text{Var}\,(\delta_2)}{\langle \delta_1 \rangle \langle \delta_2 \rangle^2} + \cdots + \frac{\text{Var}\,(\delta_m)}{\langle \delta_1 \rangle \langle \delta_2 \rangle \cdots \langle \delta_{m-1} \rangle \langle \delta_m \rangle^2}. \tag{38}$$

This expression is of general validity for single-carrier discrete multiplication processes. (Thus, it can also be used for the SCISCM SAPD when the individual stages have different values of P.) It, and variants of it, were obtained early on [7], [8], [35]. It is apparent from the sequence of denominators in (38) that the gain of the first

stage $\langle \delta_1 \rangle$ has a substantial influence on F_e; the higher this gain, the lower the contribution to the excess noise from the subsequent stages. It is this mathematical property that spurred the development of high-gain GaP-first-dynode PMT's at RCA [36].

Two useful special cases of (37) and (38) involve PMT's with identical dynodes and PMT's with a high-gain first dynode. We first assume that all m dynodes of the device are equivalent, so that the δ_k are independent and identically distributed (iid) random variables for all k, with mean and variance given by $\langle \delta \rangle$ and Var (δ), respectively. Then (37) becomes

$$\langle M \rangle = \langle \delta \rangle^m \tag{39}$$

whereas (38) becomes

$$F_e = 1 + \frac{\text{Var } (\delta)}{\langle \delta \rangle \, (\langle \delta \rangle - 1)} \left[1 - \frac{1}{\langle \delta \rangle^m} \right]. \tag{40}$$

These expressions are exact and applicable to *any* single-carrier device with m identical stages. Thus, the formula for the SCISCM SAPD excess noise factor given in (29a) may be obtained by setting $\langle \delta \rangle = 1 + P$ and Var $(\delta) = P(1 - P)$.

We next assume that all stages produce iid secondary electrons, with mean and variance $\langle \delta \rangle$ and Var (δ) respectively, *except* for the first stage for which

$$\langle \delta_1 \rangle = A \langle \delta \rangle \tag{41a}$$

and

$$\text{Var } (\delta_1) = A \text{ Var } (\delta) \tag{41b}$$

where A is a constant. When $A >> 1$, this characterizes the high-gain first-dynode PMT (e.g., GaP). The mean gain (37) then becomes

$$\langle M \rangle = A \langle \delta \rangle^m \tag{41c}$$

whereas the excess noise factor (38) becomes

$$F_e = 1 + \frac{\text{Var } (\delta)}{A \langle \delta \rangle \, (\langle \delta \rangle - 1)} \left[1 - \frac{1}{\langle \delta \rangle^m} \right]. \tag{42}$$

The similarity between (42) and (40) is obvious, with the prefactor $1/A$ on the right-hand side of (42) succinctly representing the excess-noise-factor advantage of the high-gain first-dynode tube.

To proceed further, the variance of the gain at the various stages must be specified. This is determined by the secondary-emission process at the dynodes. The simplest and most frequently used model invokes Poisson secondary-emission multiplication at every stage (Var $(\delta) = \langle \delta \rangle$) [7], [8], [35], [37]–[39]. A more versatile model is provided by the neagative-binomial (or Polya) distribution, which has been used by Prescott [40] and others [34], [41], [42]. This distribution arises from a mixture of Poisson distributions whose means are smeared in accordance with the gamma distribution [43]. Physically, the smearing is thought to arise from the variability of the secondary-emission efficiency across the surface of the dynode [34], [40]. In this case,

$$\text{Var } (\delta) = \langle \delta \rangle + \langle \delta \rangle^2 / D \tag{43}$$

where D is the "degrees-of-freedom" parameter describing the extent of the smearing [44]. Two special limits of the negative binomial are the Poisson distribution for which $D = \infty$ (the least noisy) and the Bose–Einstein (or Furry) distribution for which $D = 1$ (the most noisy).

Of the various possibilities implicit in the results of this section, the overall lowest excess noise factor obtains for a high-gain first-dynode PMT with Poisson multiplication. In that case, using (41)–(43), we obtain

$$F_e = 1 + \frac{1}{\langle M \rangle} \left[\frac{\langle M \rangle / A - 1}{(\langle M \rangle / A)^{1/m} - 1} \right]. \tag{44}$$

Equation (44) is plotted as the dashed curves in Fig. 3 for $A = 10$ ($m = 1$, 4, 10). The gain of the $m = 1$ (4) GaP PMT is approximately the same as that of the $m = 5$ (10) SAPD. It is apparent that the excess noise factor of the PMT can fall below that of the SAPD. Of course, the overall gain of a PMT can stretch to $\approx 10^8$, which is far and away greater than that achievable by any APD.

The excess noise factor for Poisson secondary-emission multiplication without the benefit of the high-gain first dynode (all dynodes identical) is obtained by setting $A = 1$ in (44). When $\langle M \rangle >> 1$, F_e then takes the well-known approximate form

$$F_e \approx \langle M \rangle^{1/m} / (\langle M \rangle^{1/m} - 1) = \langle \delta \rangle / (\langle \delta \rangle - 1), \tag{45}$$

signifying essentially noise-free multiplication even in this case.

The excess noise factor for a high-gain first-dynode PMT with Bose–Einstein secondary-electron statistics is obtained from (41)–(43) with $D = 1$. It is

$$F_e = 1 + \frac{1 + (\langle M \rangle / A)^{1/m}}{\langle M \rangle} \left[\frac{\langle M \rangle / A - 1}{(\langle M \rangle / A)^{1/m} - 1} \right], \tag{46}$$

which is plotted as the long-dash curve in Fig. 4 for $A = 10$ ($m = 10$).

Finally, the noisiest of the PMT cases considered here arises for Bose–Einstein secondary-electron statistics with all dynodes equivalent. This result is obtained by setting $A = 1$ in (46). For $\langle M \rangle >> 1$, F_e then takes the approximate form

$$\begin{aligned} F_e &\approx 2 \langle M \rangle^{1/m} / (\langle M \rangle^{1/m} - 1) \\ &= 2 \langle \delta \rangle / (\langle \delta \rangle - 1). \end{aligned} \tag{47}$$

This is only a factor of 2 greater than the excess noise factor in (45) for Poisson multiplication. This case is plotted as the short-dash curves in Fig. 4 ($m = 4$, 10).

It is apparent that, even at its noisiest, the PMT is a relatively quiet device. This is a consequence of its single-carrier vacuum character. The low excess noise factor has made the PMT an indispensible tool in optics laboratories since the 1930's and it is not likely to be relegated to the junk heap any time soon.

VII. Conclusion

We have obtained a general expression (10b) for the output-current variance of a photodetector in terms of the Fano factor of the photoelectrons $\mathcal{F}_a$ and the excess noise factor of the multiplication process intrinsic to the detector F_e. Sources of noise such as dark current, Johnson noise, and $1/f$ noise were not included in the simple formulation considered here; they can be easily incorporated, however. The analysis assumed instantaneous multiplication in that the measurement time was assumed to be greater than the time response of the signal [32].

The variance can be cast in terms of a current signal-to-noise ratio at the output of the photodetector given by

$$\begin{aligned}\text{SNR}\,(I_n) &\equiv \langle I_n\rangle/[\text{Var}\,(I_n)]^{1/2} \\ &= [\langle I_a\rangle/2qB(\mathcal{F}_a + F_e - 1)]^{1/2} \qquad (48)\end{aligned}$$

where $\langle I_a\rangle = \eta\langle I_{\text{photon}}\rangle$. In the usual situation of Poisson photon arrivals ($\mathcal{F}_a = 1$), the output-current variance is proportional to F_e in accordance with

$$\text{Var}\,(I_n) = 2q\langle I_a\rangle\, B\langle M\rangle^2 F_e \qquad (49)$$

whereupon the experimental excess noise factor is

$$\phi_e = \langle M\rangle^2 F_e \qquad (50)$$

and the SNR is

$$\text{SNR}\,(I_n) = [\langle I_a\rangle/2qBF_e]^{1/2}. \qquad (51)$$

In this case, optimization of the SNR simply involves minimizing F_e, independent of $\langle M\rangle$. In the presence of thermal noise and/or dark noise, however, optimization of the SNR is achieved at specific values of $\langle M\rangle$ and F_e.

Under conditions of Poisson photon excitation (or indeed for any distribution of photons for which $\mathcal{F}_a$ is constant and independent of $\langle a\rangle$), the right-hand side of (3) depends only on the random gain M. Thus, the ratio of overall count variance to overall count mean is constant and independent of the excitation level. The output current from any multiplying detector illuminated by such light therefore has shot-noise-like behavior. A useful consequence of this property is the applicability of the square-root normalizing transformation [45]. With the help of this computational tool, system performance can be readily evaluated in approximate form [46]. The presence of additive thermal noise and/or dark noise will, however, destroy this shot-noise-like behavior.

In the complete absence of photoelectron fluctuations ($\mathcal{F}_a = 0$), and thermal and dark noise, the output-current variance is no longer proportional to F_e, but is instead proportional to $(F_e - 1)$. Thus, Var $(I_n) \to 0$ as $F_e \to 1$. In this idealized case, the signal-to-noise ratio at the output of the photodetector is

$$\text{SNR}\,(I_n) = [\langle I_a\rangle/2qB(F_e - 1)]^{1/2}, \qquad (52)$$

which can become large for a photodetector with $F_e \to 1$.

Expressions for the excess noise factors for CAPD, SAPD, and PMT photodetectors have been set forth and graphically displayed. In terms of existing devices, small Si CAPD's with high quantum efficiency and near-ideal performance ($F_e = 2.6$ corresponding to $k_c = 0.006$ at $\langle M\rangle = 100$) have been fabricated in the wavelength region $0.4 < \lambda < 0.95$ μm [47]. Devices that are even more quiet, with $F_e < 2.2$ corresponding to $k_c < 0.002$ at $\langle M\rangle = 100$, appear to be possible [48]. CAPD devices with essentially SCISCM properties are therefore currently available at this wavelength. However, quaternary devices are generally used in the wavelength region $\lambda \approx 1.5$ μm. Unfortunately, these have $k_c \approx 1$ so that F_e is much higher [20]. Dark current and leakage current may also present difficulties in such devices.

SAPD's offer promise in this longer wavelength region. These devices have potential as small, high quantum efficiency, low-voltage photodetectors, with low leakage current [5], [20]. Although SAPD's can, in principle, exhibit minimal noise ($F_e \to 1$), their average multiplication is restricted ($\langle M\rangle \leq 2^m$ for SCISCM operation). Residual hole ionization is also a potential problem and it is imperative to construct devices in which this effect is minimized [33]. The dark-current behavior of various SAPD's has not yet been established. Attempts are currently underway to construct a long-wavelength staircase SAPD [24].

Photomultiplier tubes have remarkably low excess noise, along with the desirable properties of low dark current, high gain, good pulse resolution, and ease of operation in the photon-counting mode. However, as is well known, they suffer from limited quantum efficiency, large size, high-voltage requirements, luminescence noise, and afterpulsing due to H^+ ions or inverse photoemission [34].

PMT's are sometimes used to discriminate between single- and multiple-photoelectron events. This capability follows from the high gain as well as the narrowness of the multiplied electron distribution [34] and is associated with a minimal value of the gain Fano factor $\mathcal{F}_M$. Such discrimination is more difficult for the CAPD which suffers from a (rather broad) shifted Bose–Einstein gain distribution. It may also be difficult for the SAPD which exhibits multiple peaks in the gain distribution, unless P is close to unity [32]. A related matter is the operation of a photodetector as a high-speed photon counter. This generally requires some 10^4 electrons/photon to overcome preamplifier Johnson noise [48]. Although this is readily achieved with a PMT, such gains are not easily attained with APD's. In particular, reaching this gain in a SCISCM SAPD would require a structure of some 15 stages [48].

As a final note, we reiterate that the excess noise factor is an inadequate measure for describing the performance of a digital-signal information-transmission system. Appropriate performance measures for such systems (e.g., probability of error) require knowledge of the electron-counting distributions. In particular, digital-system performance is strongly dependent on the tails of these distributions. Certain of the photodetectors discussed here will have more favorable shapes for minimizing error probabilities than will others. This will be elucidated in a

companion study of error probabilities for a simple optical receiver, to be presented elsewhere [12].

ACKNOWLEDGMENT

We are grateful to R. J. McIntyre, F. Capasso, K. Brennan, and J. Conradi for valuable discussions.

REFERENCES

[1] J. Conradi, "The distribution of gains in uniformly multiplying avalanche photodiodes: Experimental," *IEEE Trans. Electron Devices*, vol. ED-19, pp. 713–718, 1972.

[2] R. J. McIntyre, "Multiplication noise in uniform avalanche diodes," *IEEE Trans. Electron Devices*, vol. ED-13, pp. 164–168, 1966.

[3] ——, "The distribution of gains in uniformly multiplying avalanche photodiodes: Theory," *IEEE Trans. Electron Devices*, vol. ED-19, pp. 703–713, 1972.

[4] P. P. Webb, R. J. McIntyre, and J. Conradi, "Properties of avalanche photodiodes," *RCA Rev.*, vol. 35, pp. 234–278, 1974.

[5] F. Capasso, W. T. Tsang, and G. F. Williams, "Staircase solid-state photomultipliers and avalanche photodiodes with enhanced ionization rates ratio," *IEEE Trans. Electron Devices*, vol. ED-30, pp. 381–390, 1983.

[6] K. M. van Vliet, A. Friedmann, and L. M. Rucker, "Theory of carrier multiplication and noise in avalanche devices—Part II: Two-carrier processes," *IEEE Trans. Electron Devices*, vol. ED-26, pp. 752–764, 1979.

[7] V. K. Zworykin, G. A. Morton, and L. Malter, "The secondary emission multiplier—A new electronic device," *Proc. IRE*, vol. 24, pp. 351–375, 1936.

[8] W. Shockley and J. R. Pierce, "A theory of noise for electron multipliers," *Proc. IRE*, vol. 26, pp. 321–332, 1938.

[9] G. E. Stillman and C. M. Wolfe, "Avalanche photodiodes," in *Semiconductors and Semimetals, Vol. 12, Infrared Detectors II*, R. K. Willardson and A. C. Beer, Eds. New York: Academic, 1977, pp. 291–393.

[10] S. D. Personick, "New results on avalanche multiplication statistics with application to optical detection," *Bell Syst. Tech. J.*, vol. 50, pp. 167–189, 1971.

[11] ——, "Statistics of a general class of avalanche detectors with applications to optical communication," *Bell Syst. Tech. J.*, vol. 50, pp. 3075–3095, 1971.

[12] M. C. Teich, K. Matsuo, and B. E. A. Saleh, "Counting distributions and error probabilities for optical receivers incorporating superlattice avalanche photodiodes," *IEEE Trans. Electron Devices*, to be published.

[13] R. E. Burgess, "Some topics in the fluctuation of photo-processes in solids," *J. Phys. Chem. Solids*, vol. 22, pp. 371–377, 1961.

[14] M. C. Teich and B. E. A. Saleh, "Effects of random deletion and additive noise on bunched and antibunched photon-counting statistics," *Opt. Lett.*, vol. 7, pp. 365–367, 1982.

[15] K. M. van Vliet and L. M. Rucker, "Noise associated with reduction, multiplication and branching processes," *Physica*, vol. 95A, pp. 117–140, 1979.

[16] K. Matsuo, M. C. Teich, and B. E. A. Saleh, "Poisson branching point processes," *J. Math. Phys.*, vol. 25, pp. 2174–2185, 1984.

[17] A. S. Tager, "Current fluctuations in a semiconductor (dielectric) under the conditions of impact ionization and avalanche breakdown," *Sov. Phys.—Solid State*, vol. 6, pp. 1919–1925, 1965.

[18] G. F. Williams, F. Capasso, and W. T. Tsang, "The graded bandgap multilayer avalanche photodiode: A new low-noise detector," *IEEE Electron Device Lett.*, vol. EDL-3, pp. 71–73, 1982.

[19] F. Capasso, "Band-gap engineering via graded gap, superlattice, and periodic doping structures: Applications to novel photodetectors and other devices," *J. Vac. Sci. Technol. B*, ser. 2, vol. 1, pp. 457–461, 1983.

[20] G. E. Stillman, V. M. Robbins, and N. Tabatabaie, "III-V compound semiconductor devices: Optical detectors," *IEEE Trans. Electron Devices*, vol. ED-31, pp. 1643–1655, 1984.

[21] F. Capasso, W. T. Tsang, A. L. Hutchinson, and G. F. Williams, "Enhancement of electron impact ionization in a superlattice: A new avalanche photodiode with a large ionization rate ratio," *Appl. Phys. Lett.*, vol. 40, pp. 38–40, 1982.

[22] K. Mohammed, F. Capasso, J. Allam, A. Y. Cho, and A. L. Hutchinson, "New high-speed long-wavelength $Al_{0.48}In_{0.52}As/Ga_{0.47}In_{0.53}As$ multiquantum well avalanche photodiodes," *Appl. Phys. Lett.*, vol. 47, pp. 597–599, 1985.

[23] R. Chin, N. Holonyak, G. E. Stillman, J. Y. Tang, and K. Hess, "Impact ionization in multilayered heterojunction structures," *Electron. Lett.*, vol. 16, pp. 467–469, 1980.

[24] F. Capasso, AT&T Bell Lab., Murray Hill, NJ, private communication.

[25] F-Y. Juang, U. Das, Y. Nashimoto, and P. K. Bhattacharya, "Electron and hole impact ionization coefficients in GaAs-$Al_xGa_{1-x}As$ superlattices," *Appl. Phys. Lett.*, vol. 47, pp. 972–974, 1985.

[26] H. Blauvelt, S. Margalit, and A. Yariv, "Single-carrier-type dominated impact ionisation in multilayer structures," *Electron. Lett.*, vol. 18, pp. 375–376, 1982.

[27] J. S. Smith, L. C. Chiu, S. Margalit, A. Yariv, and A. Y. Cho "A new infrared detector using electron emission from multiple quantum wells," *J. Vac. Sci. Technol. B*, vol. 1, pp. 376–378, 1983.

[28] S. L. Chuang and K. Hess, "Impact ionization across the conduction-band-edge discontinuity of quantum-well heterostructures," *J. Appl. Phys.*, vol. 59, pp. 2885–2894, 1986.

[29] F. Capasso, J. Allam, A. Y. Cho, K. Mohammed, R. J. Malik, A. L. Hutchinson, and D. Sivco, "New avalanche multiplication phenomenon in quantum well superlattices: Evidence of impact ionization across the band-edge discontinuity," *Appl. Phys. Lett.*, vol. 48, May 1986.

[30] F. Capasso, "The channeling avalanche photodiode: A novel ultra-low-noise interdigitated p-n junction detector," *IEEE Trans. Elect. Dev.*, vol. ED-29, pp. 1388–1395, 1982.

[31] K. Brennan, "Theory of the channeling avalanche photodiode," *IEEE Trans. Elect. Dev.*, vol. ED-32, pp. 2467–2478, 1985.

[32] K. Matsuo, M. C. Teich, and B. E. A. Saleh, "Noise properties and time response of the staircase avalanche photodiode," *IEEE Trans. Electron Devices*, vol. ED-32, pp. 2615–2623, 1985; also, *J. Lightwave Technol.*, vol. LT-3, pp. 1223–1231, 1985.

[33] K. Brennan, "Theory of electron and hole impact ionization in quantum well and staircase superlattice avalanche photodiode structures," *IEEE Trans. Electron Devices*, vol. ED-32, pp. 2197–2205, 1985; "Theory of GaInAs/AlInAs doped quantum-well APD: A new low-noise solid-state photodetector for light-wave communications systems," *IEEE Trans Elect. Dev.*, submitted for publication 1986.

[34] R. W. Engstrom, *RCA Photomultiplier Handbook (PMT-62)*. Lancaster, PA: RCA Electro Optics and Devices, 1980.

[35] P. M. Woodward, "A statistical theory of cascade multiplication," *Proc. Cambridge Phil. Soc.*, vol. 44, pp. 404–412, 1948.

[36] G. A. Morton and H. M. Smith, "Pulse height resolution of high gain first dynode photomultipliers," *Appl. Phys. Lett.*, vol. 13, pp. 356–357, 1968.

[37] L. Janossy, *Zh. Eksperim. Teor. Fiz.*, vol. 28, p. 679, 1955; also, "Statistical problems of an electron multiplier," *Sov. Phys.—JETP*, vol. 1, pp. 520–531, 1955.

[38] F. J. Lombard and F. Martin, "Statistics of electron multiplication," *Rev. Sci. Instrum.*, vol. 32, pp. 200–201, 1961.

[39] K. Matsuo, B. E. A. Saleh, and M. C. Teich, "Cascaded Poisson processes," *J. Math. Phys.*, vol. 23, pp. 2353–2364, 1982.

[40] J. R. Prescott, "A statistical model for photomultiplier single-electron statistics," *Nucl. Instrum. Meth.*, vol. 39, pp. 173–179, 1966.

[41] G. Lachs, "The statistics for the detection of light by nonideal photomultipliers," *IEEE J. Quantum Electron.*, vol. QE-10, pp. 590–596, 1974.

[42] C. W. Helstrom, "Output distributions of electrons in a photomultiplier," *J. Appl. Phys.*, vol. 55, pp. 2786–2792, 1984.

[43] M. Greenwood and G. U. Yule, "An inquiry into the nature of frequency distributions representative of multiple happenings with particular reference to the occurrence of multiple attacks of disease or of repeated accidents," *J. Royal Statist. Soc.*, ser. A., vol. 83, pp. 255–279, 1920.

[44] B. E. A. Saleh, *Photoelectron Statistics*. Berlin/Heidelberg/New York: Springer-Verlag, 1978.

[45] P. R. Prucnal and M. C. Teich, "Multiplication noise in the human visual system at threshold: 2. Probit estimation of parameters," *Biol. Cybern.*, vol. 43, pp. 87–96, 1982.

[46] P. R. Prucnal and B. E. A. Saleh, "Evaluation of fiber-optic error rates using a normalizing transform," *J. Opt. Soc. Amer.*, vol. 72, pp. 1171–1178, 1982.

[47] P. P. Webb and R. J. McIntyre, "Recent developments in silicon avalanche photodiodes," *RCA Eng.*, vol. 27, pp. 96–102, 1982.

[48] R. J. McIntyre, RCA Electro-Optics Photodetectors, Ste. Anne de Bellevue, P.Q., Canada, personal communication.

Malvin C. Teich (S'62–M'66–SM'72) was born in New York, NY. He received the S.B. degree in physics from the Massachusetts Institute of Technology, Cambridge, in 1961, the M.S. degree in electrical engineering from Stanford University, Stanford, CA, in 1962, and the Ph.D. degree in quantum electronics from Cornell University, Ithaca, NY, in 1966.

In 1966 he joined the M.I.T. Lincoln Laboratory, Lexington, MA, where he was engaged in work on coherent infrared detection. In 1967 he became a member of the faculty in the Department of Electrical Engineering, Columbia University, New York, NY, where he is now teaching and pursuing his research interests in the areas of optical and infrared detection, quantum optics, lightwave communications, and sensory perception. He served as Chairman of the Department from 1978 to 1980. He is also a member of the faculty in the Department of Applied Physics and Nuclear Engineering, and a member of the Columbia Radiation Laboratory, the Center for Telecommunications Research, and the Columbia Bioengineering Institute. He has authored or coauthored some 100 technical publications and holds one patent.

Dr. Teich is a member of Sigma Xi, the American Physical Society, the Acoustical Society of America, the Society for Neuroscience, the American Association for the Advancement of Science, and the New York Academy of Sciences. He served as a member of the Editorial Advisory Panel for *Optics Letters* from 1977 to 1979. In 1969 he was the recipient of the IEEE Browder J. Thompson Memorial Prize for his paper "Infrared Heterodyne Detection" and in 1981 he received the Citation Classic Award of *Current Contents* for this work. He was appointed a Fellow of the John Simon Guggenheim Memorial Foundation in 1973 and was elected a Fellow of the Optical Society of America in 1983.

Kuniaki Matsuo (M'85) was born in Hiroshima, Japan. He received the B.S. degree in electrical engineering from Tokyo Electrical Engineering College, Tokyo, in 1972 and the M.S. and Ph.D. degrees in electrical engineering from Columbia University, New York, NY, in 1978 and 1984, respectively.

From 1984 to 1986 he was a Postdoctoral Research Scientist in the Columbia Radiation Laboratory, Department of Electrical Engineering, Columbia University. In 1986 he joined the Hiroshima-Denki Institute of Technology, Hiroshima, Japan, where he is now teaching and pursuing his research interests in avalanche photodetection, quantum electronics, and point processes.

Dr. Matsuo is a member of Sigma Xi.

Bahaa E. A. Saleh (M'73) received the B.S. degree from Cairo University, Cairo, Egypt, in 1966 and the Ph.D. degree from The Johns Hopkins University, Baltimore, MD, in 1971, both in electrical engineering.

From 1971 to 1974 he was an Assistant Professor at the University of Santa Catarina, Brazil. Thereafter, he joined the Max Planck Institute, Göttingen, Germany, where he was involved in research in laser light scattering and photon correlation spectroscopy. He is presently Professor of Electrical and Computer Engineering at the University of Wisconsin, Madison, where he has been since 1977. He held visiting appointments at the University of California, Berkeley, in 1977, and the Columbia Radiation Laboratory of Columbia University in 1983. He is currently involved in research in image processing, optical information processing, statistical optics, optical communication, and vision. He is the author of *Photoelectron Statistics* (Springer, 1978) and a co-editor of *Transformations in Optical Signal Processing* (SPIE, 1981). In 1980–1983 he was an Associate Editor of the *Journal of the Optical Society of America*, and since 1983 he has been a Topical Editor of the same journal.

Dr. Saleh is a Fellow of the Optical Society of America and a member of Phi Beta Kappa and Sigma Xi. He was one of the recipients of the 1984–1985 Guggenheim Fellowship.